Physics Letters B 785 (2018) 90–94

Contents lists available at ScienceDirect

Physics Letters B

www.elsevier.com/locate/physletb

$\Lambda^*(1405)$-matter: Stable or unstable?

J. Hrtánková [a,b], N. Barnea [c], E. Friedman [c], A. Gal [c,*], J. Mareš [a], M. Schäfer [a,b]

[a] Nuclear Physics Institute, 25068 Řež, Czech Republic
[b] Faculty of Nuclear Sciences and Physical Engineering, Czech Technical University in Prague, 115 19 Prague 1, Czech Republic
[c] Racah Institute of Physics, The Hebrew University, 91904 Jerusalem, Israel

ARTICLE INFO

Article history:
Received 29 May 2018
Received in revised form 20 July 2018
Accepted 2 August 2018
Available online 24 August 2018
Editor: J. Hisano

Keywords:
Strange matter
$\Lambda^*(1405)$ resonance
Kaonic atoms
RMF

ABSTRACT

A recent suggestion by Akaishi and Yamazaki (2017) [3] that purely-$\Lambda^*(1405)$ nuclei provide the absolute minimum energy in charge-neutral baryon matter for baryon-number $A \gtrsim 8$, is tested within RMF calculations. A broad range of Λ^* interaction strengths, commensurate with $(\bar{K}\bar{K}NN)_{I=0}$ binding energy assumed to be of order 100 MeV, is scanned. It is found that the binding energy per Λ^*, B/A, saturates for $A \gtrsim 120$ with values of B/A considerably below 100 MeV, implying that $\Lambda^*(1405)$ matter is highly unstable against strong decay to Λ and Σ hyperon aggregates. The central density of Λ^* matter is found to saturate as well, at roughly twice nuclear matter density. Moreover, it is shown that the underlying very strong $\bar{K}N$ potentials, fitted for isospin $I = 0$ to the mass and width values of $\Lambda^*(1405)$, fail to reproduce values of single-nucleon absorption fractions deduced across the periodic table from K^- capture-at-rest bubble chamber experiments.

1. Introduction

Strangeness ($\mathcal{S}$) provides for extension of standard nuclear matter to strange matter in which SU(3)-octet hyperons (Λ, Σ, Ξ) may prove as abundant as nucleons [1]. Particularly interesting at present is the role of hyperons in the composition of the neutron star interior, the so called 'hyperon puzzle' [2]. Little is known about the possible role of higher-mass hyperons in hadronic matter. However, it was recently suggested by Akaishi and Yamazaki (AY) [3] that purely-$\Lambda^*(1405)$ aggregates become increasingly bound with the number $A = -\mathcal{S}$ of Λ^* constituents, reaching absolute stability for $A \gtrsim 8$. This suggestion for which we found no documented supporting calculations beyond $A = 2$ follows a similar conjecture made already in 2004 [4]. It is worth recalling that solving the A-body Schrödinger equation for purely attractive $\Lambda^*\Lambda^*$ interactions will necessarily lead to collapse, with the binding energy per Λ^*, B/A, and the central Λ^* density $\rho(r \approx 0)$ diverging as A increases. This immediately raises the question whether AY perhaps just overlooked this basic many-body aspect of the Schrödinger equation in asserting that purely-Λ^* matter becomes absolutely stable for some given value of A. Therefore the issue of stability has to be checked within calculational schemes that avoid many-body collapse. A commonly used approach in nuclear and hadronic physics that avoids collapse and provides sufficiently faithful reproduction of nuclear binding energies and densities is the Relativistic Mean Field (RMF) approach [5] which is used here.

In this Letter, we show within RMF calculations in which strongly attractive $\Lambda^*\Lambda^*$ interactions are generated through scalar meson (σ) and vector meson (ω) exchanges that both B/A, the Λ^*-matter binding energy per baryon, and the central density $\rho(r \approx 0)$ saturate for values of A of order $A \sim 100$. For the case considered here, B/A saturates at values between roughly 30 to 80 MeV, depending on details of the RMF modeling, and the associated central densities saturate at values about twice nuclear-matter density. This leaves Λ^* aggregates highly unstable against strong interaction decay governed by two-body conversion reactions such as $\Lambda^*\Lambda^* \to \Lambda\Lambda, \Sigma\Sigma$.

The plan of this note is as follows. In Sect. 2 we briefly review several few-body calculations of $\bar{K}$ nuclear quasibound states, including those based on energy independent strongly attractive $\bar{K}N$ potentials as advocated by AY, in order to introduce plausible input values for the $\Lambda^*\Lambda^*$ binding energy ($B_{\Lambda^*\Lambda^*}$) used to determine the strength of the scalar and vector meson-exchange couplings applied in our subsequent RMF calculations. In Sect. 3 we question the validity of such energy independent strongly attractive $\bar{K}N$ interactions by checking their ability to reproduce the single-nucleon absorption fractions deduced from K^- capture observations in bubble chamber experiments. RMF calculations of purely-Λ^* nuclei are reported in Sect. 4, showing clearly how B/A

* Corresponding author.
E-mail address: avragal@savion.huji.ac.il (A. Gal).

https://doi.org/10.1016/j.physletb.2018.08.031

Table 1
$(\bar{K}N)_{I=0}$, $(\bar{K}NN)_{I=1/2}$ and $(\bar{K}\bar{K}NN)_{I=0}$ binding energies B (in MeV) calculated using energy dependent (E-dep.) [9] and energy independent (E-indep.) [10] $\bar{K}N$ potentials. $(\bar{K}\bar{K}NN)_{I=0}$ binding energies are transformed in the last row to $B_{\Lambda^*\Lambda^*}$ values.

$\bar{K}$ nuclei	(E-dep.)	$(\text{E-indep.})_a$	$(\text{E-indep.})_b$
$(\bar{K}N)_{I=0}$	11.4	26.6	64.2
$(\bar{K}NN)_{I=1/2}$	15.7	51.5	102
$(\bar{K}\bar{K}NN)_{I=0}$	32.1	93	190
$\Lambda^*\Lambda^*$	9.3	40	62

and ρ saturate as a function of A, thereby leaving Λ^* matter highly unstable. A brief Conclusion section summarizes our results with some added discussion.

2. $\bar{K}$ nuclear quasibound states

The $I = 0$ antikaon–nucleon $(\bar{K}N)$ interaction near threshold is attractive and sufficiently strong to form a quasibound state. Using a single-channel energy independent $\bar{K}N$ potential this quasibound state has been identified by AY, e.g. in Refs. [6,7], with the $J^P = (1/2)^-$ $\Lambda^*(1405)$ resonance about 27 MeV below the K^-p threshold. In contrast, in effective field theory (EFT) approaches where the $\bar{K}N$ effective single-channel potential comes out energy dependent, reflecting the coupling to the lower-energy $\pi\Sigma$ channel, this $\bar{K}N$ quasibound state is bound only by about 10 MeV [8]. The difference between $\bar{K}N$ binding energies gets compounded in multi-$\bar{K}N$ quasibound states predicted in these two approaches, as demonstrated for $(\bar{K}\bar{K}NN)_{I=0}$ in Table 1 by comparing binding energies B listed in the (E-dep.) column with those listed in the (E-indep.) columns. Regarding these two columns, we note that the binding energies listed in column $(\text{E-indep.})_b$ arise by fitting the $(\bar{K}N)_{I=0}$ potential strength such that it reproduces the value $B(\bar{K}NN)_{I=1/2} = 102$ MeV derived from the DISTO experiment [11]. This derivation was challenged subsequently by the HADES Collaboration [12]. The most recent J-PARC E15 [13] dedicated experiment derives a value of $B(\bar{K}NN)_{I=1/2} = 47 \pm 3^{+3}_{-6}$ MeV. Therefore, when studying energy independent $\bar{K}N$ potentials, we will keep to the $(\text{E-indep.})_a$ scenario that also identifies the $(\bar{K}N)_{I=0}$ quasibound state with the $\Lambda^*(1405)$ resonance observed 27 MeV below threshold. This identification plays an essential role in the earlier Akaishi and Yamazaki works, Refs. [6,7]. It is worth noting that the more refined state-of-the-art chiral EFT approaches, with low-energy constants fitted to *all* existing K^-p low-energy data, produce two $(\bar{K}N)_{I=0}$ quasibound states [14], the narrower and least bound of which is consistent with the (E-dep.) column of Table 1.

3. Kaonic atoms test

Here we confront the $(\text{E-indep.})_a$ scenario of the last section with the broad data base of kaonic atoms which are known to provide a sensitive test of $\bar{K}N$ interaction models near threshold [15]. In the last decade several chiral EFT models of the $\bar{K}N$ interaction provided K^-N scattering amplitudes based on fits to low energy K^-p data, including kaonic hydrogen from the SIDDHARTA experiment [16,17]. Kaonic atom potentials based on such single-nucleon amplitudes within a sub-threshold kinematics approach are generally unable to fit the kaonic atom data unless an additional phenomenological density dependent amplitude representing multi-nucleon processes is introduced. In a recent work [18] this procedure was applied to several chiral EFT $\bar{K}N$ model amplitudes. Good fits to the data were reached with χ^2 values of 110 to 120 for 65 data points. Considering that the data come

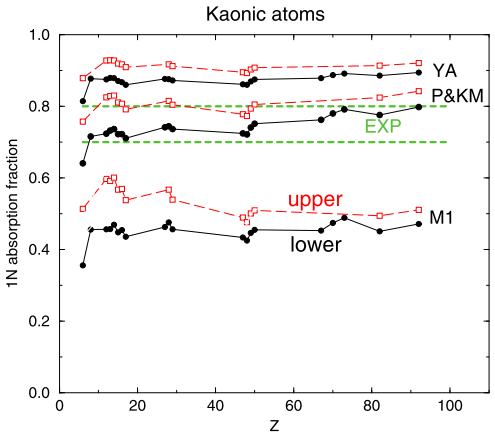

Fig. 1. K^- single-nucleon absorption fractions calculated using K^-N amplitudes from the chiral EFT models M1, P and KM, see Ref. [18], and as generated from Eq. (1) (here marked YA). The range of experimentally deduced fractions, 0.70–0.80, is marked by horizontal dashed lines; see Ref. [18] for a comment on carbon (lowest Z points).

from four different laboratories, covering the whole of the periodic table, these χ^2 values are quite satisfactory. This procedure was extended to include also $\bar{K}N$ amplitudes generated from the energy independent $\bar{K}N$ potentials used by Yamazaki and Akaishi (YA) [7] (in MeV),

$$V^{I=0}_{\bar{K}N}(r) = (-595 - \text{i}83)\exp[-(r/0.66\ \text{fm})^2],$$
$$V^{I=1}_{\bar{K}N}(r) = (-175 - \text{i}105)\exp[-(r/0.66\ \text{fm})^2]. \quad (1)$$

These potentials approximate reasonably the $(\text{E-indep.})_a$ scenario of the last section. The corresponding $\bar{K}N$ amplitudes are shown in Fig. 15 of Ref. [19].[1] Like other models, also this model fails to fit kaonic atoms data on its own. Adding a phenomenological density dependent amplitude produces fits with χ^2 of 150 for the 65 data points, which is significantly inferior to fits obtained for the chiral EFT models considered in Ref. [18].

It was shown in Ref. [18] that one could distinguish between different $\bar{K}N$ models by testing their ability to reproduce experimentally deduced values of single-nucleon absorption fractions at threshold across the periodic table. Fig. 1 shows such fractions as calculated for four models of the $\bar{K}N$ interaction, including that of Eq. (1). Results of calculated absorptions from the so-called lower state and whenever provided by measured yields also from the upper state are shown for each kaonic atom. Experiments [20–22] do not distinguish directly between the two types of absorption.

As shown in the figure the $\bar{K}N$ interaction model of Eq. (1) (marked by YA) leads to far too large single-nucleon fractions whereas, for example, the Murcia (M1) model leads to too small ratios. The Kyoto–Munich (KM) model and the Prague (P) model, which yield predictions indistinguishable from each other, provide a very good agreement with experiment. The bottom line for the present discussion is that the $\bar{K}N$ interaction model of Eq. (1) does not reproduce the experimental absorption fractions.

4. RMF calculations of purely-Λ^* nuclei

Bound systems of Λ^* hyperons are treated here in a similar way as applied to nuclei [5] and also to hypernuclei, e.g. in Ref. [23], within the RMF framework. In our calculations of Λ^* nuclei, we employed the linear RMF model HS [24], taking into account the

[1] We thank Tetsuo Hyodo for providing us with tables of these amplitudes.

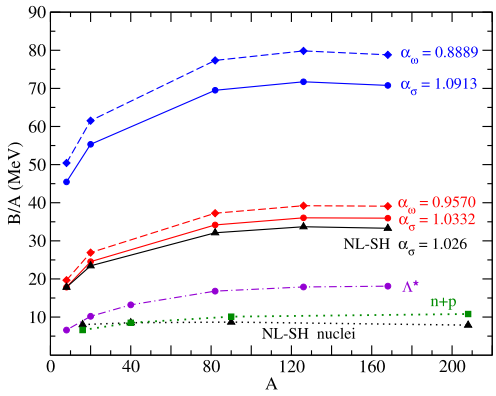

Fig. 2. Binding energy of Λ^* nuclei per Λ^*, B/A as a function of mass number A, calculated within the HS and NL-SH RMF models for various strengths of scalar and vector fields (see text for details). The binding energy per nucleon in atomic nuclei is shown for comparison ($n+p$: HS without Coulomb and ρ meson field, NL-SH nuclei: including these terms).

coupling of Λ^* baryons to isoscalar–scalar σ and isoscalar–vector ω meson fields. Other fields considered in ordinary nuclei, such as isovector–vector $\vec{\rho}$ or Coulomb fields were disregarded since the Λ^* is a neutral $I=0$ baryon. The resulting RMF model Lagrangian density for Λ^* nuclei is of the form ($\hbar = c = 1$ from now on):

$$\mathcal{L} = \bar{\Lambda}^* \left[\mathrm{i}\gamma^\mu D_\mu - (M_{\Lambda^*} - g_{\sigma\Lambda^*}\sigma) \right] \Lambda^* + (\sigma, \omega_\mu \text{ free-field terms}), \tag{2}$$

where the covariant derivative $D_\mu = \partial_\mu + \mathrm{i}\, g_{\omega\Lambda^*}\, \omega_\mu$ couples the vector meson field ω to the Λ^* baryon fields. Here we disregard the $\omega\Lambda^*$ tensor coupling term $f_{\omega\Lambda^*}\sigma_{\mu\nu}\omega_\nu$ which, while affecting spin–orbit splittings of single-particle levels, has little effect on the total binding energies of closed-shell nuclear systems (or Λ^* nuclei).

To start with, we used the HS linear model for atomic nuclei [24] with scalar and vector meson masses m_i ($i = \sigma, \omega$) and coupling constants g_{iN} given by

$$m_\sigma = 520\ \text{MeV},\quad m_\omega = 783\ \text{MeV},\quad g_{\sigma N} = 10.47,\quad g_{\omega N} = 13.80. \tag{3}$$

Modifying these coupling constants in ways described below, we explored Λ^* nuclei with closed shells by solving self-consistently the coupled system of the Klein–Gordon equations for meson fields and the Dirac equation for Λ^*.

In Fig. 2 we show binding energy values per baryon, B/A, calculated as a function of A for atomic nuclei (lowest two lines) and for purely Λ^* nuclei using mostly the linear HS model. It is clear that B/A saturates in all shown cases for $A \gtrsim 120$, to a value of order 10 MeV for nucleons when using parameters specified in Eq. (3), and to a somewhat higher value in the case of Λ^* nuclei (marked by Λ^*) upon using the same parameters. The increased B/A values in this case with respect to atomic nuclei is due to the higher Λ^* mass which reduces its kinetic energy. This is not yet the Λ^* matter calculation we should pursue since when extrapolated to $A=2$ it gives a $B_{\Lambda^*\Lambda^*}$ value of only a few MeV, whereas the calculation pursued here assumes a considerably stronger $\Lambda^*\Lambda^*$ binding corresponding to $B(\bar{K}\bar{K}NN)_{I=0} - 2B(\bar{K}N)_{I=0} \approx 40$ MeV from column (E-indep.)$_a$ in Table 1.[2] To renormalize the Λ^* RMF calculation to

[2] We note for comparison that the scalar and vector Λ^* couplings estimated in the microscopic calculations of Ref. [28] within a chiral EFT model do not produce a bound $\Lambda^*\Lambda^*$ state.

Table 2
Values of the scaling parameters α_σ and α_ω for σ and ω fields, respectively, each yielding $B_{\Lambda^*\Lambda^*} = 40$ MeV.

$V_{\Lambda^*\Lambda^*}$	α_σ	α_ω
Dover–Gal (4)	1.0332	0.9750
Machleidt (5)	1.0913	0.8889

such a high value of $B_{\Lambda^*\Lambda^*}$ we need to increase $g_{\sigma N}$ or decrease $g_{\omega N}$ from the values listed in Eq. (3). This is how the other B/A lines marked by scaling factors α_σ or α_ω in Fig. 2 are obtained. The appropriate values of α_σ and α_ω are determined as follows.

The RMF underlying attractive scalar (σ) exchange and repulsive vector (ω) exchange baryon–baryon (BB) spin-singlet $S=0$ potentials are given to lowest order in $(m/M)^2$ recoil corrections, disregarding tensor couplings, by:

$$V_{BB}(r) = g^2_{\omega B}\,(1 - \frac{3}{8}\frac{m^2_\omega}{M^2_B})\,Y_\omega(r) - g^2_{\sigma B}\,(1 - \frac{1}{8}\frac{m^2_\sigma}{M^2_B})\,Y_\sigma(r) \tag{4}$$

according to Dover–Gal [26], or

$$V_{BB}(r) = g^2_{\omega B}\,Y_\omega(r) - g^2_{\sigma B}\,(1 - \frac{1}{4}\frac{m^2_\sigma}{M^2_B})\,Y_\sigma(r) \tag{5}$$

according to Machleidt [27]. Here $Y_i(r) = \exp(-m_i r)/(4\pi r)$ is the Yukawa form for meson exchange. The difference in the $(m/M)^2$ recoil terms in these two forms arises from a total neglect of nonlocal contributions in Dover–Gal, while partially retaining them by Machleidt. Using these BB $= \Lambda^*\Lambda^*$ potentials, with $M_{B=\Lambda^*} =$ 1405 MeV, $\Lambda^*\Lambda^*$ binding energies were calculated by solving a two-body Schrödinger equation, scaling either $g_{\sigma N}$ or $g_{\omega M}$ according to $g_{\sigma N} \to g_{\sigma\Lambda^*} = \alpha_\sigma g_{\sigma N}$ and $g_{\omega N} \to g_{\omega\Lambda^*} = \alpha_\omega g_{\omega N}$ so as to get $B_{\Lambda^*\Lambda^*} = 40$ MeV while retaining the other coupling constant fixed. The resulting scaling parameters are listed in Table 2.

We then performed RMF calculations of Λ^* nuclei using the renormalized coupling constants as marked to the right of each line in Fig. 2. Saturation is robust in all versions for $A \gtrsim 120$, but the saturation value depends on which potential version is used, Dover–Gal (4) or Machleidt (5). Scaling the ω meson coupling results in larger values of Λ^* binding energies than by scaling the σ meson coupling. Calculations were also performed using the nonlinear RMF model NL-SH [25] for comparison. The corresponding scaling parameter $\alpha_\sigma = 1.026$ was fitted to yield the binding energy of the $8\Lambda^*$ system calculated within the HS model for $\alpha_\sigma = 1.0332$. The resulting NL-SH calculation yields similar binding energies per Λ^* to those produced in the linear HS model. Fig. 2 clearly demonstrates that B/A does not exceed 100 MeV in any of the versions studied here. The calculated values are without exception considerably lower than the ≈ 290 MeV required to reduce the $\Lambda^*(1405)$ mass in the medium below that of the lightest hyperon $\Lambda(1116)$. This conclusion remains valid when Λ^* absorption is introduced in the present RMF calculations, say by considering the two-body conversion processes $\Lambda^*\Lambda^* \to YY$ ($Y = \Lambda,\ \Sigma$). Absorption normally translates into effective repulsion in bound state problems, thereby reducing the total binding energy and hence also the associated B/A values in Λ^* nuclei.

Having shown that B/A values saturate in Λ^* nuclei to values less than 100 MeV, we illustrate in Fig. 3 that the central density $\rho(r \approx 0)$ also saturates as a function of the mass number A. This is demonstrated in the left panel for the NL-SH model and $\alpha_\sigma = 1.026$. The central densities $\rho(0)$ shown in the figure vary in the range of 0.3–0.45 fm^{-3}, which is about twice nuclear matter density. Expressing the r.m.s. radius of the Λ^* nuclear density distribution ρ as $r_{\rm rms} = r_0\, A^{\frac{1}{3}}$, the variation of the radius parameter r_0 with A is shown in the right panel of the figure for selected

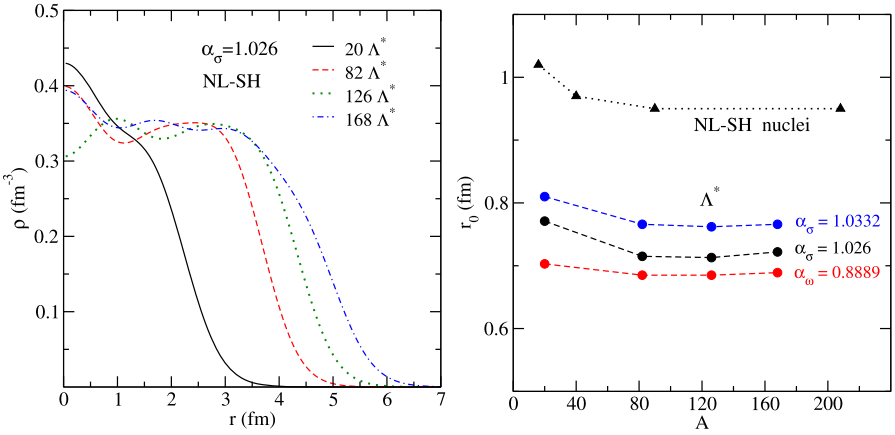

Fig. 3. Left: Λ^* density distribution in systems composed of 20, 82, 126 and 168 Λ^* baryons, calculated within the NL-SH RMF model for $\alpha_\sigma = 1.026$. Right: values of the r.m.s. radius parameter r_0 in Λ^* nuclei (see text) for three of the RMF models and interaction strengths giving rise to B/A lines in Fig. 2. Values of r_0 in atomic nuclei (marked 'NL-SH nuclei') calculated within the NL-SH model are shown for comparison.

$\Lambda^*\Lambda^*$ potential versions. Again, the radii r_0 saturate with values about 0.7–0.8 fm, indicating that Λ^* nuclei are more compressed than atomic nuclei in which r_0 is typically 0.9–1.0 fm, as shown by the upper line. The approximate constancy of r_0 with A is consistent with approximately uniform Λ^* matter density.

5. Conclusion

It was shown within a straightforward RMF calculation that the $\Lambda^*(1405)$ stable-matter scenario promoted by AY [3] is unlikely to be substantiated in standard many-body schemes. The decisive role of Lorentz covariance to produce saturation in the RMF calculations of binding energies and sizes reported in Sect. 4 is worth noting. Lorentz covariance introduces two types of baryon density, a scalar $\rho_S = \bar{B}B$ associated with the attractive σ meson field and a vector $\rho_V = \bar{B}\gamma_0 B$ associated with the repulsive ω meson field. Whereas ρ_V coincides with the conserved baryon density $B^\dagger B$ (denoted simply ρ on the l.h.s. of Fig. 3), ρ_S shrinks with respect to ρ_V in dense matter by a multiplicative factor $M^*/E^* < 1$, where $M^* = M - g_{\sigma B}\langle\sigma\rangle < M$ is the baryon density-dependent effective mass, thereby damping the attraction from the scalar σ meson field [5]. Saturation in the RMF model is thus entirely a relativistic phenomenon. Calculations within the non-relativistic approach with static potentials such as (4) or (5) would lead to collapse of systems composed of sufficiently large number of Λ^* baryons, as it also holds for nucleons [29].

Doubts were also raised in the present work on the validity of using a very strong and energy-independent $\bar{K}N$ $I = 0$ dominated potential fitted directly to the position and width of the $\Lambda^*(1405)$ resonance. Similar potentials have been used by AY over the years to promote the case for strongly bound $\bar{K}$ nuclear clusters, see Table 1 here, and thereby also to suggest strongly attractive $\Lambda^*\Lambda^*$ interactions that would according to them lead to absolutely stable Λ^* matter. It was shown in Sect. 3 here that such strong and energy-independent $\bar{K}N$ potentials do not pass the test of kaonic atoms, hence casting doubts on their applicability in describing higher density kaonic features. Having said it, we concede that a proper description of high density hadronic matter, considerably beyond the $\rho \approx 2\rho_0$ density regime reached in our own calculations, may require the introduction of additional, new interaction mechanisms such as proposed recently in Ref. [30].

Finally, we recall related RMF calculations of multi-$\bar{K}$ nuclei [31] in which, for a given core nucleus, the resulting $\bar{K}$ separation energy $B_{\bar{K}}$, as well as the associated nuclear and $\bar{K}$-meson densities, were found to saturate with the number of $\bar{K}$ mesons ($\gtrsim 10$). Saturation appeared in that study robust against a wide range of variations, including the RMF nuclear model used and the type of boson fields mediating the strong interactions. In particular strange systems made of protons and K^- mesons, as similar as possible to aggregates of $\Lambda^*(1405)$ baryons, were found in that work to be less bound than other strange-matter configurations. Our findings are in good qualitative agreement with the conclusion reached there that the SU(3) octet hyperons (Λ, Σ, Ξ) provide, together with nucleons, for the lowest energy strange hadronic matter configurations [1].

Acknowledgements

J.H. and M.S. acknowledge financial support from the CTU-SGS Grant No. SGS16/243/OHK4/3T/14. The work of N.B. is supported by the Pazy Foundation and by the Israel Science Foundation grant No. 1308/16.

References

[1] J. Schaffner, C.B. Dover, A. Gal, C. Greiner, H. Stöcker, Phys. Rev. Lett. 71 (1993) 1328;
J. Schaffner, C.B. Dover, A. Gal, C. Greiner, D.J. Millener, H. Stöcker, Ann. Phys. 235 (1994) 35;
J. Schaffner-Bielich, A. Gal, Phys. Rev. C 62 (2000) 034311.
[2] D. Chatterjee, I. Vidaña, Eur. Phys. J. A 52 (2016) 29.
[3] Y. Akaishi, T. Yamazaki, Phys. Lett. B 774 (2017) 522.
[4] T. Yamazaki, Y. Akaishi, A. Doté, Phys. Lett. B 587 (2004) 167.
[5] B.D. Serot, J.D. Walecka, Adv. Nucl. Phys. 16 (1986) 1, preceded by a more compact and accessible form in Phys. Lett. B 87 (1979) 172.
[6] Y. Akaishi, T. Yamazaki, Phys. Rev. C 65 (2002) 044005.
[7] T. Yamazaki, Y. Akaishi, Phys. Rev. C 76 (2007) 045201.
[8] T. Hyodo, D. Jido, Prog. Part. Nucl. Phys. 67 (2012) 55.
[9] N. Barnea, A. Gal, E.Z. Liverts, Phys. Lett. B 712 (2012) 132.
[10] S. Maeda, Y. Akaishi, T. Yamazaki, Proc. Jpn. Acad. Ser. B 89 (2013) 418.
[11] T. Yamazaki, et al., Phys. Rev. Lett. 104 (2010) 132502.
[12] G. Agakishiev, et al., Phys. Lett. B 742 (2015) 242.
[13] S. Ajimura, et al., arXiv:1805.12275 [nucl-ex], submitted for publication to Phys. Rev. Lett.
[14] U.-G. Meißner, T. Hyodo, Pole structure of the Λ(1405) region, a PDG18 Review in M. Tanabashi, et al., Phys. Rev. D 98 (2018) 030001.
[15] E. Friedman, A. Gal, Phys. Rep. 452 (2007) 89.
[16] M. Bazzi, et al., SIDDHARTA Collaboration, Phys. Lett. B 704 (2011) 113.
[17] M. Bazzi, et al., SIDDHARTA Collaboration, Nucl. Phys. A 881 (2012) 88.
[18] E. Friedman, A. Gal, Nucl. Phys. A 959 (2017) 66.
[19] T. Hyodo, W. Weise, Phys. Rev. C 77 (2008) 035204.
[20] H. Davis, et al., Nuovo Cimento A 53 (1968) 313.
[21] J.W. Moulder, et al., Nucl. Phys. B 35 (1971) 332.
[22] C. Vander Velde-Wilquet, et al., Nuovo Cimento A 39 (1977) 538.
[23] J. Mareš, B.K. Jennings, Phys. Rev. C 49 (1994) 2472.
[24] C.J. Horowitz, B.D. Serot, Nucl. Phys. A 368 (1981) 503.

[25] M.M. Sharma, M.A. Nagarajan, P. Ring, Phys. Lett. B 312 (1993) 377.
[26] C.B. Dover, A. Gal, Prog. Part. Nucl. Phys. 12 (1984) 171.
[27] R. Machleidt, Adv. Nucl. Phys. 19 (1989) 189.
[28] T. Uchino, T. Hyodo, M. Oka, Nucl. Phys. A 868–869 (2011) 53.
[29] M. Schäfer, et al., work in preparation.
[30] W. Paeng, M. Rho, Phys. Rev. C 91 (2015) 015801.
[31] D. Gazda, E. Friedman, A. Gal, J. Mareš, Phys. Rev. C 77 (2008) 045206.